Semi-nonlinear waveguides for three waves mixing

Romain Morleghem[1], Simone Napolitano[4] and Stéphane Clemmen[1,2,3]

[1]Laboratoire d'Information Quantique, CP 225, Université libre de Bruxelles (U.L.B.), Belgium
[2]OPERA-Photonique, CP 194/5, Université libre de Bruxelles (U.L.B.), Brussels, Belgium
[3]Photonics Research Group, Department of Information Technology, Ghent University-imec, Belgium
[4]Experimental Soft Matter and Thermal Physics (EST), Université libre de Bruxelles, Brussels, Belgium

Abstract

Silicon nitride (SiN) has emerged as a mature photonics platform due to its very low losses and large transparency but lacks a significant $\chi^{(2)}$ nonlinearity [1]. Hence, the integration of ultra-high $\chi^{(2)}$ thin films on SiN waveguides, resulting in so-called semi-nonlinear waveguides, would open the way for many functionalities such as second harmonic (SH) generation and single photons frequency conversion [2]. We design semi-nonlinear waveguides that achieve modal phase matching between a spatially fundamental mode (TE_{00}) at an initial frequency and a spatially 2 lobe-mode (TE_{01}) at the SH [3]. We thoroughly compare the predicted SH conversion efficiency in that situation to usual situation of a fully nonlinear waveguide requiring phase matching between the same TE_{00} mode and the TE_{20} mode at the SH (the lowest possible order of non-vanishing modal phase matching). Our simulations show that semi-nonlinear waveguides result in a higher SH conversion efficiency than fully nonlinear waveguides.

Silicon nitride platform and hybrid integration with $\chi^{(2)}$ materials

Silicon nitride (SiN) is a mature and versatile platform, exhibiting a lot of attractive features for integrated nonlinear and quantum photonics: a high bandgap (transparent down to 400 nm), very low losses (~ 0.1 dB/cm) and state-of-the-art $\chi^{(3)}$ platform [4]. Still, SiN lacks a $\chi^{(2)}$ nonlinearity due to its centrosymmetric structure, preventing the SiN platform from key $\chi^{(2)}$ applications like high-speed electro-optic modulation and frequency conversion (sum/difference frequency generation).

Although it is possible to induce an effective $\chi^{(2)}_{eff}$ in SiN by several methods (strain, electric field, all-optical poling [5], …), the resulted $\chi^{(2)}_{eff}$ and on-chip SH conversion efficiency are several orders of magnitude lower than material platforms possessing an intrinsic $\chi^{(2)}$ coefficient [5].

Another strategy consists in the integration of a high $\chi^{(2)}$ material on existing SiN waveguides, resulting in a semi-nonlinear structure as depicted in figure 1. Several materials already used to fabricate nanophotonics circuits like $LiNbO_3$, AlN, SiC, GaP, InGaP [6] are potential candidates for this hybrid integration with SiN. However, the aforementioned $\chi^{(2)}$ materials are not ideal for different reasons: AlN and SiC have a relatively low $\chi^{(2)}$ coefficient (not exceeding 20 pm/V). The very high tensorial component $\chi^{(2)}_{xyz}$ of GaP and InGaP (~ 200 pm/V) is difficult to exploit effectively. The ferroelectric $LiNbO_3$ constitute arguably the state-of-the-art because its etching has reached a certain maturity resulting in very low loss waveguides and it also offers possibilities of phase matching via periodic poling. Yet, $LiNbO_3$ is far from being perfect for processes such as sum frequency generation because of the limitations associated to a photorefractive effect and a moderate $\chi^{(2)}$ (55 pm/V). Besides those $\chi^{(2)}$ semiconductor materials, organic materials like OH1(2-(3-(4-hydroxystyryl)-5,5-dimethylcyclohex-2-

enylidene)malononitrile) and BNA (N-benzyl-2-methyl-4-nitroaniline) fulfill the required features for the hybrid integration with SiN waveguides : a transparency range extending in the visible and near infrared, a bandgap high enough to avoid linear and two photons absorption at telecom wavelength, a $\chi^{(2)}$ coefficient significantly higher than that of $LiNbO_3$ (bulk $\chi^{(2)}$ ~ 150-250 pm/V), a refractive index closed to the one of SiN (~2) and finally, a convenient processability and good thermal stability. BNA thin films exhibiting a $\chi^{(2)}$ of the order of 150 pm/V at 1550 nm have already been demonstrated [7] but the control of their processing conditions and their interfacing to existing SiN integrated circuits is currently lacking. Thus, the integration of a ultra-high organic $\chi^{(2)}$ thin film (BNA or OH1) on top of SiN waveguides would undoubtedly transform the SiN platform into an all-nonlinear photonics champion.

Second harmonic generation via modal phase matching

The $\chi^{(2)}$ response is usually assessed using second harmonic generation (SHG), where an input fundamental wave at ω (1550 nm) is upconverted to a second harmonic wave at 2ω (775 nm). Moreover, to have an efficient SH conversion, the fundamental and second harmonic need to be phase matched, i.e., travel at the same phase velocity. This phase matching condition is fulfilled when the effective refractive index of the fundamental and the SH mode equal each other — n(ω) = n(2ω). Yet, due to dispersion, the effective refractive index increases with frequency for a given spatial mode of the waveguide. The modal phase matching strategy is based on having the SH wave in a higher order spatial mode, allowing to have n(ω) = n(2ω). In practice, modal phase matching is achieved by carefully engineering the geometric dimensions of the waveguide, which add up to 3 parameters in our case: the SiN core width and thickness as well as the $\chi^{(2)}$ overlay thickness. For this $\chi^{(2)}$ overlay, we investigate first the organic BNA whose highest tensorial component is the $\chi^{(2)}_{xxx}$ as depicted on figure 1, which means that the spatial modes involved are (quasi) TE modes. A key advantage of the semi-nonlinear structure is the use of the first higher order TE_{01} mode for the SH wave (assuming a fundamental TE_{00} mode). The TE_{01} mode can easily be excited using on-chip mode converters [8]. As depicted in the top left inset of figure 3, the SH TE_{01} mode consists of 2 vertically stacked lobes: a negative-valued lobe lying in the SiN core and a positive-valued lobe lying in the BNA overlay. Having only one lobe in the $\chi^{(2)}$ overlay allows to reach significant nonlinear modal overlap integral, and consequently high SH conversion efficiency as it has already been experimentally demonstrated using semi-nonlinear $TiO_2/LiNbO_3$ waveguides [3].

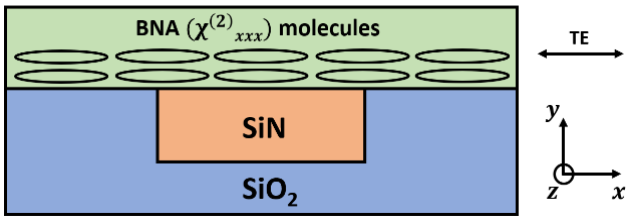

Figure 1: Semi-nonlinear waveguide made of a SiN core and a high $\chi^{(2)}$ overlay. The $\chi^{(2)}$ thin film is based on a crystalline arrangement of organic BNA molecules oriented along the x direction. Therefore, this high $\chi^{(2)}_{xxx}$ component can be exploited by using TE modes for the fundamental and second harmonic waves.

Second harmonic conversion efficiency in semi-nonlinear waveguides

As evidence of the suitability of those new semi-nonlinear waveguides in nonlinear photonics, we theoretically compare (assuming modal phase matching) the SH

conversion efficiency between semi-nonlinear SiN/BNA waveguides (SH in TE_{01}) to the simpler situation of a hypothetical monolithic BNA waveguide requiring phase matching in the TE_{20} (or TE_{02}) SH mode in order to have a non-vanishing overlap with the fundamental TE_{00} mode. This SH conversion efficiency map is depicted in figure 2 and further explained in the caption. This map shows that, within a certain range of geometric dimensions, the best waveguides are the semi-nonlinear ones, which is mostly due to a higher confinement of the two phase matched waves.

In figure 3, we plot the theoretical SH conversion efficiency as a function of the $\chi^{(2)}$ nonlinearity of the BNA thin films. The bulk $\chi^{(2)}$ of BNA has been reported to 160 pm/V at a fundamental wavelength of 1550 nm [9], shown by a vertical dotted line on figure 3. On the same figure, we also add the theoretical SH conversion efficiency of state-of-the-art $LiNbO_3$ waveguides (PPLN [10,11] and dual layer thin film $LiNbO_3$ [12]). Thanks to the very high nonlinearity of BNA (almost 3 times the one of $LiNbO_3$), it is predicted that these semi-nonlinear SiN/BNA waveguides lead to SH conversion efficiency much higher than the ones of current PPLN waveguides.

In conclusion, we have theoretically demonstrated that ultra-high $\chi^{(2)}$ semi-nonlinear SiN/BNA waveguides lead to much higher SH conversion efficiency compared to their fully nonlinear counterparts and current PPLN waveguides. The next step in our analysis is to consider tolerances to fabrication (variation of waveguide dimensions), in order to estimate the phase matching bandwidth of the SHG process.

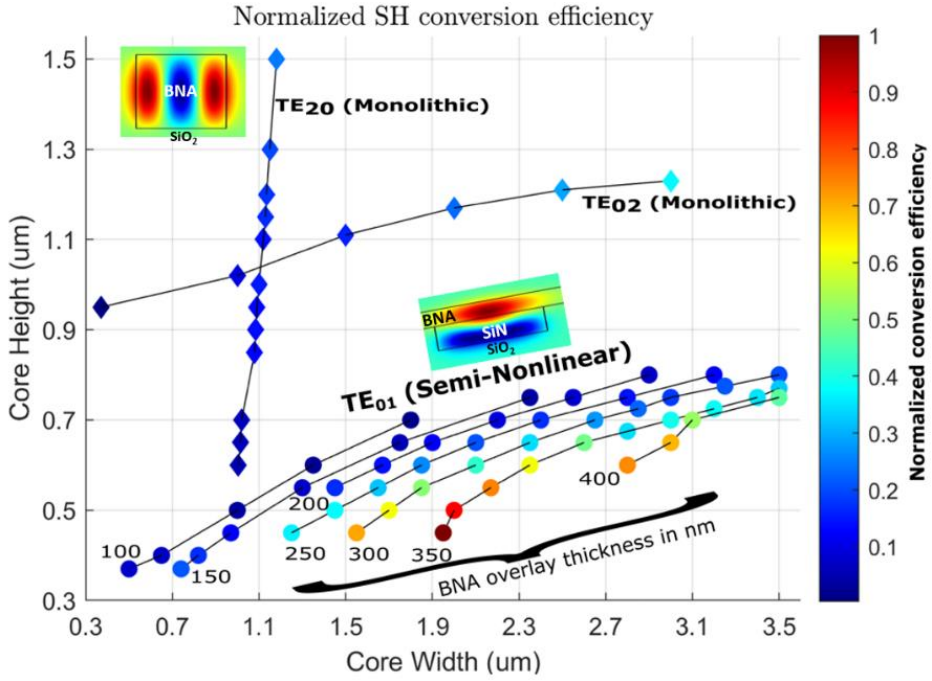

Figure 2: Second harmonic conversion efficiency map (1550 nm → 775 nm) for monolithic (diamond) and semi-nonlinear modal phase matched waveguides (circle). The core dimensions correspond to the $\chi^{(2)}$ core (BNA) for the monolithic case and to the SiN core for the semi-nonlinear case. The values near the TE_{01}(semi-nonlinear) curves correspond to the BNA overlay thickness (in nm) for the semi-nonlinear case. The conversion efficiency is normalized by the highest value found in the simulation (29000 % $W^{-1}cm^{-2}$ for the waveguide with SiN width = 1.95 um / SiN height = 450 nm / BNA height = 350 nm). In the SH mode profiles (TE_{20} mode for monolithic and TE_{01} mode for semi-nonlinear), red (blue) lobes correspond to a positive (negative) field value.

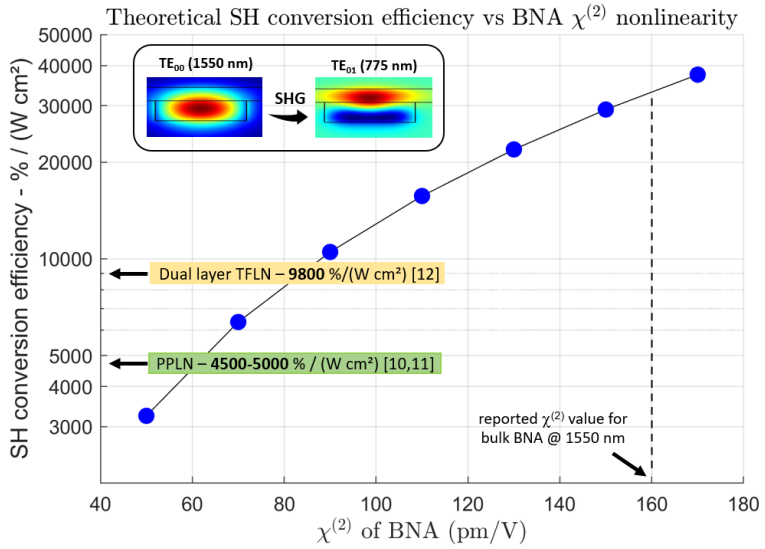

Figure 3: Theoretical second harmonic (SH) conversion efficiency (in % $W^{-1}cm^{-2}$) plotted as a function of the $\chi^{(2)}$ nonlinearity of the BNA overlay (circles). The semi-nonlinear waveguide (SiN core with BNA overlay) with the mode profiles are depicted in the top left inset of the figure. We also report on the graph the bulk $\chi^{(2)}$ of BNA (~ 160 pm/V at 1550 nm) on the horizontal axis as well as state-of-the-art theoretical SH conversion efficiency with $LiNbO_3$ ($\chi^{(2)}$ ~ 55 pm/V) waveguides on the vertical axis. Thanks to the very high nonlinearity of BNA (almost 3 times the one of $LiNbO_3$), these semi-nonlinear SiN/BNA waveguides outperform nanophotonics $LiNbO_3$ waveguides with respect to the theoretical SH conversion efficiency.

Acknowledgement Stéphane Clemmen is a research associate of the Fonds De La Recherche Scientifique — FNRS. This work was supported by the Fonds de la Recherche Scientifique – FNRS under Grant MIS F.4506.20.

References

[1] Abdul Rahim et al. "Expanding the silicon photonics portfolio with silicon nitride photonic integrated circuits". In: Journal of lightwave technology 35.4 (2017), pp. 639–649.
[2] Anaıs Dréau et al. "Quantum frequency conversion of single photons from a nitrogen-vacancy center in diamond to telecommunication wavelengths". In: Physical review applied 9.6 (2018), p. 064031.
[3] Rui Luo et al. "Semi-nonlinear nanophotonic waveguides for highly efficient second-harmonic generation". In: Laser & Photonics Reviews 13.3 (2019), p. 1800288.
[4] Xingchen Ji et al. "Exploiting ultralow loss multimode waveguides for broadband frequency combs". In: Laser & Photonics Reviews 15.1 (2021), p. 2000353.
[5] Edgars Nitiss et al. "Optically reconfigurable quasi-phase-matching in silicon nitride microresonators". In: Nature Photonics 16.2 (2022), pp. 134–141.
[6] Galan Moody et al. "2022 Roadmap on integrated quantum photonics". In: Journal of Physics: Photonics 4.1 (2022), p. 012501.
[7] Artur Hermans et al. "Growth of organic crystalline thin films with strong second-order nonlinearity for integrated optics". In: 21st European Conference on Integratred Optics (ECIO 2019).
[8] Aseema Mohanty et al. "Quantum interference between transverse spatial waveguide modes". In: Nature communications 8.1 (2017), pp. 1–7.
[9] Takashi Notakel et al. "Ultra-precise processing and Maker fringe measurements of organic N-Benzyl-2-Methyl-4-Nitroaniline crystal". In: 2018 43rd International Conference on Infrared, Millimeter, and Terahertz Waves (IRMMW-THz). IEEE. 2018, pp. 1–2.
[10] Cheng Wang et al. "Ultrahigh-efficiency wavelength conversion in nanophotonic periodically poled lithium niobate waveguides". In: Optica 5.11 (2018), pp. 1438–1441.
[11] Ashutosh Rao et al. "Actively-monitored periodic-poling in thin-film lithium niobate photonic waveguides with ultrahigh nonlinear conversion efficiency of 4600% W- 1 cm- 2". In: Optics express 27.18(2019), pp. 25920–25930.
[12] Lei Wang, Xiuquan Zhang, and Feng Chen. "Efficient Second Harmonic Generation in a Reverse Polarization Dual-Layer Crystalline Thin Film Nanophotonic Waveguide". In: Laser & Photonics Reviews 15.12 (2021), p. 2100409.